Mitigating a century of European renewable variability with transmission and informed siting

Wohland, Jan; Brayshaw, David; Pfenninger, Stefan

DOI
10.1088/1748-9326/abff89

Publication date
2021

Document Version
Final published version

Published in
Environmental Research Letters

ENVIRONMENTAL RESEARCH
LETTERS

LETTER • OPEN ACCESS

Mitigating a century of European renewable variability with transmission and informed siting

ENVIRONMENTAL RESEARCH
LETTERS

LETTER

Mitigating a century of European renewable variability with transmission and informed siting

Jan Wohland[1,*], David Brayshaw[2] and Stefan Pfenninger[1,3]

[1] Climate Policy Group, Institute for Environmental Decisions, ETH Zürich, Zürich, Switzerland
[2] Department of Meteorology, University of Reading, Reading, United Kingdom
[3] Faculty of Technology, Policy and Management (TPM), Delft University of Technology, Delft, The Netherlands
[*] Author to whom any correspondence should be addressed.

E-mail: jwohland@ethz.ch

Keywords: renewable energy, wind energy, solar energy, climate variability, transmission infrastructure, climate change mitigation, multidecadal variability

Supplementary material for this article is available online

OPEN ACCESS

RECEIVED
8 December 2020

REVISED
5 May 2021

ACCEPTED FOR PUBLICATION
10 May 2021

PUBLISHED
24 May 2021

Abstract

To reach its goal of net greenhouse gas neutrality by 2050, the European Union seeks to massively expand wind and solar power. Relying on weather-dependent power generation, however, poses substantial risks if climate variability is not adequately understood and accounted for in energy system design. Here we quantify European wind and solar generation variability over the last century, finding that both vary on a multidecadal scale, but wind more strongly. We identify hotspots and study dominant patterns of (co-)variability, finding that solar generation varies mostly uniformly across Europe while the leading wind variability modes reveal cross-border balancing potential. Combined wind and solar power generation in the current European system exhibits multidecadal variability of around 5% and can be further reduced through European cooperation or locally optimized wind shares, albeit the latter comes at the expense of significantly enhancing seasonal to interannual variability. Improved spatial planning therefore offers multiple options to mitigate long-term renewable generation variability but requires careful assessments of the trade-offs between climate-induced variations on different timescales.

1. Introduction

By 2050, the European Commission aims to achieve net greenhouse gas neutrality and considers renewables to play an essential role in eliminating emissions (European Commission 2019). Yet power generation from wind turbines and solar cells is weather-dependent, complicating their integration into the energy system (Bloomfield *et al* 2016, 2021, Collins *et al* 2018, van der Wiel *et al* 2019). Strategic siting of generators (Grams *et al* 2017, Santos-Alamillos *et al* 2017), optimized portfolios of different types of generation (Heide *et al* 2010) and large-scale transmission (Rodríguez *et al* 2014) are key mechanisms to mitigate generation variability on the supply side.

The atmosphere features variability on many scales (Williams *et al* 2017) and is connected to other climate subsystems that induce long-term variability such as the oceans (Keenlyside *et al* 2015, Farneti 2017). Quantifying long-term resource availability of renewable power generation matters because wind parks and solar systems are operated over many years and need to reliably contribute to future zero emission power systems. There are two known relevant climate processes in this context. First, dimming and brightening refers to a decline in surface solar radiation from 1950 to 1980 followed by a recovery in the next decades (Wild 2016). Second, stilling describes downwards trends in near-surface wind speeds over land in the period 1980–2008 (Vautard *et al* 2010). While stilling was initially thought to be mainly driven by increased surface roughness (Wever 2012), recent evidence of surface wind speed recovery since 2010 suggests a connection to multidecadal climate variability instead (Zeng *et al* 2019).

The majority of current renewable energy modelling relies on 3D reconstructions of the atmosphere, so called reanalyses, covering the satellite period (around 1980 to today), and is consequently blind to long-term resource variability extending beyond

the past four decades (Pfenninger and Staffell 2016, Staffell and Pfenninger 2016, González-Aparicio *et al* 2017). Nevertheless, previous studies demonstrate the importance of multi-decadal wind or solar generation variability based on station measurements (Müller *et al* 2014), satellite data (Sweerts *et al* 2019), and 20th century reanalyses (Bett *et al* 2017, Wohland *et al* 2019b). The current knowledge, however, is fragmented due to earlier foci on single technologies and/or small domains. In particular, the co-variability of wind and solar power generation on long timescales or the effectiveness of transmission infrastructure to smooth multidecadal variability have not yet been thoroughly investigated despite their potentially pivotal role in future net zero power systems.

Climate data quality and reliability are major obstacles for long-term renewable resource assessments. In fact, the provision of reliable climate information over the entire twentieth century is a challenge that current centennial reanalyses fail to always meet (Befort *et al* 2016, Bloomfield *et al* 2018, Meucci *et al* 2020). Not a single current centennial reanalysis provides both plausible wind and surface radiation estimates (Wohland *et al* 2019a, 2020), complicating combined solar and wind power assessments. However, their weaknesses have been traced back to observational issues and methodological assumptions. First, centennial reanalyses from the European Centre for Medium Range Weather Prediction (ECMWF) feature spurious wind trends because the assimilated wind speed data already contains these trends (Wohland *et al* 2019a). Trends in observational marine wind speeds were extensively studied and are largely due to an evolving measurement technique (Cardone *et al* 1990, Ward and Hoskins 1996). After trend removal, all centennial reanalyses agree on long-term wind generation variability. Second, centennial reanalyses from the National Oceanic and Atmospheric Administration (NOAA) and the Cooperative Institute for Research in Environmental Sciences (CIRES) do not capture dimming and brightening because they use constant aerosols (Wohland *et al* 2020).

2. Methods and data

While individual centennial reanalysis fail to provide plausible wind and solar radiation data, their weaknesses can be overcome by informed combination of multiple reanalyses. We base input dataset selection on their performance in representing wind speeds and surface radiation on multidecadal timescales, suggesting that NOAA's Twentieth Century Reanalysis version 3 (20CRv3; Slivinski *et al* 2019) is a good choice to understand wind variability while ECMWF's coupled reanalysis of the twentieth century (CERA20C; Laloyaux *et al* 2018) captures surface radiation variability well (Bloomfield *et al* 2018, Wohland *et al* 2019a, 2020). In this study, we combine both reanalyses in a way that fully maintains internal consistency on short timescales of hours to months while capturing dimming and brightening and avoiding spurious wind trends.

To quantify uncertainty, we use the full CERA20C ensemble (ten members) and, after verifying that ensemble spread is small, choose a 20CRv3 subsample that captures the full sea surface temperature (SST) forcing spread (members 1–8, the remaining members 9–80 were forced with the same set of SSTs). We use the CERA20C forecast fields for 100 m wind speeds and surface solar radiation downwards because only one of them is also available as an analysis field. Choosing the forecast in both cases thus has the advantage of using two consistent fields (rather than using two fields that were processed differently). Both datasets have three hourly resolution and cover at least the period 1901–2010. Spatial resolution is slighlty different, and CERA20C ($1.125° \cdot 1.125°$) has a coarser grid compared to 20CRv3 ($0.5° \cdot 0.5°$). We use data on the highest common temporal and spatial resolution, permitting us to capture the daily weather cycle and resolve the main orographic features such as mountain ranges and islands.

2.1. Plausibility-checked twentieth century renewable generation

To provide internally consistent and physically plausible, non-interrupted PV and wind power generation over a century, which we call 'plausibility-checked' timeseries, we follow a two-step approach:

2.1.1. Low-frequency correction of CERA20C wind speeds

We use CERA20C as our main data source and compute both wind and solar generation from it, thereby ensuring that short-term variability is synchronous. However, the CERA20C long-term wind trends require correction. We therefore subtract the long-term variability from CERA20C and substitute with the one from 20CRv3:

$$s'_{\mathrm{CERA20C}}(\boldsymbol{x},t,i) = s_{\mathrm{CERA20C}}(\boldsymbol{x},t,i) + \underbrace{\left[\langle s_{\mathrm{20CRv3}}(\boldsymbol{x},t,j_{\mathrm{rep}})\rangle - \langle s_{\mathrm{CERA20C}}(\boldsymbol{x},t,i_{\mathrm{rep}})\rangle\right]}_{\text{correction}}, \quad (1)$$

where s'_{CERA20C} (s_{CERA20C}) denotes the corrected (uncorrected) CERA20C wind speeds calculated from the 100 m wind components in CERA20C, s_{20CRv3} are 20CRv3 wind speeds that were remapped bilinearly on the CERA20C grid, and $i \in 1..8$ is the CERA20C ensemble member. Time and location are referred to as t and $\boldsymbol{x}$, respectively. The brackets $\langle . \rangle$ denote Lanczos filtering over 4.5 years and we only report the corrected wind speeds where the filter is fully defined. We evaluated the correction term for all possible 80 combinations of CERA20C and 20CRv3 ensemble members at three latitude bands (approx. at 35°N, 46°N, 58°N) and found that the mean spread is generally smaller than 0.1 $\mathrm{m\,s^{-1}}$ which is considerably smaller than other sources of uncertainty and can be safely neglected (details in supplementary information A (available online at stacks.iop.org/ERL/16/064026/mmedia)). We therefore identified representative members $i_{\mathrm{rep}} = 7$ and $j_{\mathrm{rep}} = 5$ as the median members of their respective ensemble.

2.1.2. Conversion to wind and solar power generation

The conversion to power generation relies on established and open source methods, namely the Global Solar Energy Estimator (Pfenninger and Staffell 2016) and the windpowerlib (Haas *et al* 2019), assessing the influence of panel geometry, and capturing the full spread of currently available wind turbines. We consider three different wind turbines: the E-126/7580, SWT120/3600 and SWT142/3150. They were identified using all >2.5 MW turbines from windpowerlib (Haas *et al* 2019) as those turbines with the lowest, median and highest normalized generation at 7 $\mathrm{m\,s^{-1}}$ wind speed (details in supplementary information B). Power curves are smoothed to account for subgrid-scale turbulence using the approach detailed in Knorr (2016) and a turbulence intensity TI = 0.1246 (see figure B2).

The solar power model GSEE was modified to be more robust around sunset. In the initial implementation, direct normal radiation

$$\mathrm{dni} \propto \frac{1}{\cos(\mathrm{solar\_zenith}(t_{\mathrm{help}}))}, \tag{2}$$

experienced a singularity at sunset (solar_zenith = 90°). The three-hourly solar irradiance input data in combination with the helper time variable $t_{\mathrm{help}} = t +$ 30 mins, lead to distorted daily profiles and arch-like spatial structures in winter capacity factor maps. The new approach uses additional intermediate timesteps and calculates the mean of $\frac{1}{\cos}$ contributions, not allowing for solar zenith angles > 87° when the Sun is about to set and PV generation is therefore essentially zero anyway.

GSEE is driven with surface radiation (total and direct) and temperature data. This combination provides a methodological challenge because both are reported at the same time step but have substantially different meaning. While radiation is reported as a cumulative variable (i.e. the 9 AM radiations is the sum from 6 AM to 9 AM), temperature is instantaneous. As PV generation is highly sensitive to the position of the Sun, we decided to shift radiation data by half a timestep, thereby making it a centered mean, and to interpolate temperature linearly to the new timesteps. As a consequence, wind and solar power generation are off by 90 min which does not matter in the subsequent steps as they focus on longer time scales.

Following Pfenninger and Staffell (2016), we define three panel orientation scenarios. *Constant panel geometry* refers to constant tilt (25°) and azimuth (180°) angles. *Variable azimuth* uses the same constant tilt but azimuth angles are drawn from a Gaussian (mean 180°, standard deviation 40°). *Variable azimuth and tilt* uses tilt and azimuth angles drawn from Gaussians (azimuth: mean 180°, standard deviation 40°; tilt: mean 25°, standard deviation 15°).

We are ultimately interested in the amplitude of generation variability which we compute from the maximum (minimum) generations G_{max} (G_{min}) as

$$\mathrm{amplitude} = \frac{G_{\mathrm{max}} - G_{\mathrm{min}}}{G_{\mathrm{min}}}. \tag{3}$$

Division with the minimum generation was chosen to ease interpretation as, for example, an amplitude of 10% implies that G_{max} is 10% larger than G_{min}.

2.2. Univariate and multivariate EOF analysis

We use univariate and multivariate empirical orthogonal function (EOF) analysis to identify leading modes of spatio-temporal renewable generation variability. EOF analysis decomposes spatiotemporal input data into temporally varying principle components and spatially varying patterns by solving an eigenvalue problem, and often allows for substantial complexity reductions when large variance shares can be explained using only a few EOFs (Storch and Zwiers 1999, van den Dool 2007). We use the implementation by Dawson (2016).

2.3. Optimization of wind and solar shares on different timescales

In the optimization, wind turbines are chosen following the principle to build the biggest turbine that is suitable at a location given the wind conditions:

$$\hat{CF}_w(\boldsymbol{x},t) = \begin{cases} CF_{\text{w, E-126\_7580}}(\boldsymbol{x},t) & \text{, if } \langle CF_{\text{w, E-126\_7580}}\rangle \geqslant \theta_1 \\ CF_{\text{w, SWT120\_3600}}(\boldsymbol{x},t) & \text{, if } \langle CF_{\text{w, E-126\_7580}}\rangle < \theta_1 \text{ and } \langle CF_{\text{w, SWT120\_3600}}\rangle \geqslant \theta_2 \\ CF_{\text{w, SWT142\_3150}}(\boldsymbol{x},t) & \text{, if } \langle CF_{\text{w, E-126\_7580}}\rangle < \theta_1 \text{ and } \langle CF_{\text{w, SWT120\_3600}}\rangle < \theta_2 \text{ and } \langle CF_{\text{w, SWT142\_3150}}\rangle \geqslant \theta_3 \\ 0 & \text{, otherwise} \end{cases} \tag{4}$$

where $CF_{w,k}(\boldsymbol{x},t)$ denotes the wind capacity factor for turbine k and $\langle\rangle$ is the 20 year mean from 1980 to 2000. The thresholds are chosen as $\theta_1 = 0.3, \theta_2 = 0.25$, $\theta_3 = 0.2$. For solar PV, we only use the constant panel geometry scenario and exclude offshore domains and those with very low solar potentials ($\theta_s = 0.1$):

$$\hat{CF}_s(\boldsymbol{x},t) = \begin{cases} CF_{\text{s, constant}}(\boldsymbol{x},t) & \text{, if } \langle CF_{\text{s, constant}}\rangle \geqslant \theta_s \text{and location onshore} \\ 0 & \text{, otherwise.} \end{cases} \tag{5}$$

We group adjacent countries together to obtain country combinations with sufficiently large areas of at least 80 grid boxes (see table 1). To account for offshore wind energy, we include the exclusive economic zones. Only using suitable locations as defined above, we assume that installed capacity $C_{w,s}$ is uniform within each domain. We argue that this simplification is justified as we focus on large-scale resource variability rather than realistic high-resolution expansion planning. Mean wind capacity factors in a domain can thus be written as

$$CF_{\text{w, domain}} = \langle \hat{CF}_w \rangle_{\text{domain}}, \tag{6}$$

where $\langle\rangle_{\text{domain}}$ denotes the spatial mean. We define solar generation $CF_{\text{s, domain}}$ analogously.

Total domain-wide wind and solar generation G_{domain} thus only depends on the wind share $\alpha \in (0,1)$ and total installed capacity $C_{\text{installed}}$ as

$$G_{\text{domain}} = C_{\text{installed}} [\alpha \cdot CF_{\text{w, domain}} + (1-\alpha) \cdot CF_{\text{s, domain}}]. \tag{7}$$

We normalize generation per domain by division with its long-term mean as we are interested in the relative evolution of the combined wind-and-solar generation rather than absolute values. The normalization ensures that total long-term power generation remains unchanged when the wind share α is modified despite differences in wind and solar capacity factors. Note that the relative changes in G_{domain} are independent of the installed capacity, and thus also do not depend on the electricity consumption and the renewable shares in a country group. The wind share is optimized using two different approaches:

(a) **Minimize seasonal to interannual variability** by minimizing the standard deviation of normalized G_{domain} using 20 years of monthly data 1980–2000
(b) **Minimize multidecadal variability** by minimizing the standard deviation of normalized G_{domain} using eighty years of twenty-year running mean smoothed annual data (1917–1997, full duration over which smoothing is well defined)

which yields two different wind capacity shares (seasonal α_{season} and multidecadal α_{longterm}). Approach a mimics the current state of the art of using relatively short climatic input data that captures monthly, seasonal and interannual variability in capacity allocation optimization. Due to the dominant role of the seasonal cycle, we refer to the approach as 'seasonal' for ease of reading even though it encompasses multiple temporal scales. The state-of-the-art is contrasted with the longer-term assessment of approach b which we refer to as multidecadal, where we chose to follow Wohland *et al* (2019b) in averaging over 20y which corresponds to the reasonable lifetime of wind parks and solar panels.

2.4. Spatial balancing assessment

We investigate spatial balancing potential between the country groups using different scenarios of the wind β^w_{domain} and solar β^s_{domain} installed capacity shares. The shares are defined relative to the European wind plus solar installed capacity

$$C_{\text{Europe}} = \sum_{\text{domain}} (C^w_{\text{domain}} + C^s_{\text{domain}}) \tag{8}$$

as

$$\beta^{w,s}_{\text{domain}} = \frac{C^{w,s}_{\text{domain}}}{C_{\text{Europe}}}. \quad (9)$$

Total European generation is consequently defined as

$$G_{\text{Europe}} = C_{\text{Europe}} \sum_{\text{domain}} [\beta^{w}_{\text{domain}} \cdot CF_{\text{w, domain}} + \beta^{s}_{\text{domain}} \cdot CF_{\text{s, domain}}]. \quad (10)$$

Generation in an individual country group (isolated) and in Europe excluding a country group (others) are obtained by modifying C_{Europe} and the sum accordingly. Note that we report relative amplitudes throughout this study which is not affected by changes in the total installed capacity C_{Europe}.

We use 2019 values for installed wind and solar capacities $C^{w,s}_{\text{domain}}$ (IRENA 2020). The continent-wide wind to solar capacity ratio is 60% to 40% and capacity is unevenly distributed across the continent (see SI table I1 for more details). We define the autarky penalty as the difference between the capacity weighted mean amplitude of multidecadal variability and the European multidecadal amplitude under cooperation.

To study the effects of different design choices independently, we construct three scenario groups:

(a) In the *Current capacity and distribution* scenario group, there are three sub-scenarios. *Both* corresponds to the combined wind and solar generation fleet as it existed in 2019. *Wind* (*Solar*) corresponds to the wind (solar) fleet only, keeping the relative shares between countries unaffected.
(b) The *Current capacity and even plant distribution* group consists of three sub-scenarios that leave the continental wind to solar capacity ratio unchanged while modifying the distribution between countries. While the *Even wind* (*Even solar*) scenario distributes wind generation evenly over the country groups (each one getting $\frac{1}{9}$ of European wind(solar) capacity), the *Even both* scenario assumes that both wind and solar are distributed evenly.
(c) Lastly, the *Current plant distribution and adjusted wind share* scenarios change the continent-wide wind and solar shares while keeping the inter-country distribution unchanged. The *40% wind* scenario assumes a 20% reduction of the wind share while the *80% wind* assumes a 20% increase.

3. Results

3.1. Multidecadal changes stronger for wind than solar power

We find that both wind and solar generation feature multidecadal variability irrespective of the chosen turbine or panel geometry (see figure 1). Wind shows multiple variability hotspots, for example, off the Portuguese coast, where the biggest turbine E-126_7580 experiences more than 15% difference between the strongest and weakest 20 year period, in the English Channel, and over Sweden. Particularly strong variability also occurs in Southern Norway, but may be of limited practical relevance due to low mean capacity factors in the area. In contrast, the offshore area northwest of Great Britain features exceptionally stable multidecadal generation characteristics. Dependent on long-term capacity factors, we classify wind sites as low quality ($0.15 < CF < 0.25$), medium quality ($0.25 < CF < 0.35$) and high quality ($0.35 < CF < 0.45$). Larger turbines are impacted more strongly by multidecadal wind changes as illustrated by increased likelihoods of large multidecadal amplitudes. For instance, the likelihood of multidecadal variability in excess of 10% is approximately 10% higher for the biggest turbine (E-126_7580) at medium and high quality sites as compared to the other two turbine models (see figures 2(b) and (c)). The trend to build ever larger turbines thus comes at the cost of increased multidecadal wind generation variability.

Multidecadal solar variability is weaker than wind variability. We group solar photovoltaic locations as low quality ($0.1 < CF < 0.15$), medium quality ($0.15 < CF < 0.2$) and high quality ($0.2 < CF < 0.25$). While virtually all sites feature multidecadal wind variability greater than 4% irrespective of the chosen turbine (figures 2(a)–(c)), the same threshold is never crossed at high quality PV sites (figure 2(f)), rarely crossed at medium quality PV sites (figure 2(e)), and crossed at 80% of the low quality PV sites (figure 2(d)). The relative amplitude of multidecadal solar variability shows negligible changes under varying panel tilt and azimuth angles. We will consequently only report the scenario with constant panel geometry.

For solar power, there is a distinct latitude dependence in variability that is inversely related to latitude dependence of capacity factors. While surface radiation generally increases further south, the relative amplitude of multidecadal variability decreases towards the south. Continent-wide, the best areas for solar photovoltaics are therefore those least affected by multidecadal variability (figures 2(d)–(f)). 80% of low quality sites feature multidecadal amplitudes of 6% or less and 80% of high quality sites feature multidecadal amplitudes of 2% or less. The amplitude of multidecadal generation variability also declines with site quality for wind, but the relationship is much weaker (see figures 2(a)–(c)): the 80th percentile only drops from 11% to 10% for the biggest turbine when comparing low quality and high quality wind sites.

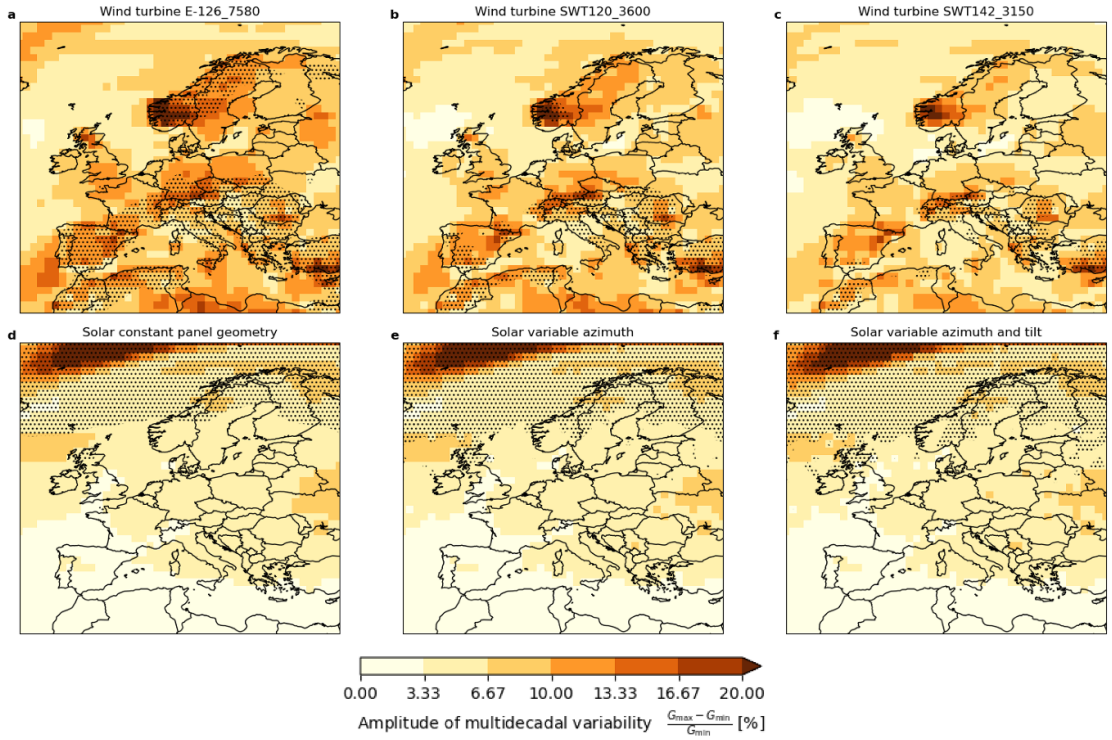

Figure 1. Hotspots of multidecadal wind (a)–(c) and solar (d)–(f) generation variability using different turbines and solar panel geometries. G_{max} (G_{min}) denote the maximum (minimum) of 20y running mean generation G. Hatching marks areas with capacity factors lower than 0.15 (wind) or 0.1 (solar). Values denote the ensemble mean. Wind turbines (E-126_7580, SWT120_3600, SWT142_3150) in a-c were chosen to sample the full performance range of currently available turbines (see SI section B). Solar constant panel geometry refers to constant tilt (25°) and azimuth (180°) angles. Solar variable azimuth uses the same constant tilt but azimuth angles are drawn from a Gaussian (mean 180°, standard deviation 40°). Solar variable azimuth and tilt uses tilt and azimuth angles drawn from Gaussians (azimuth: mean 180°, standard deviation 40°; tilt: mean 25°, standard deviation 15°).

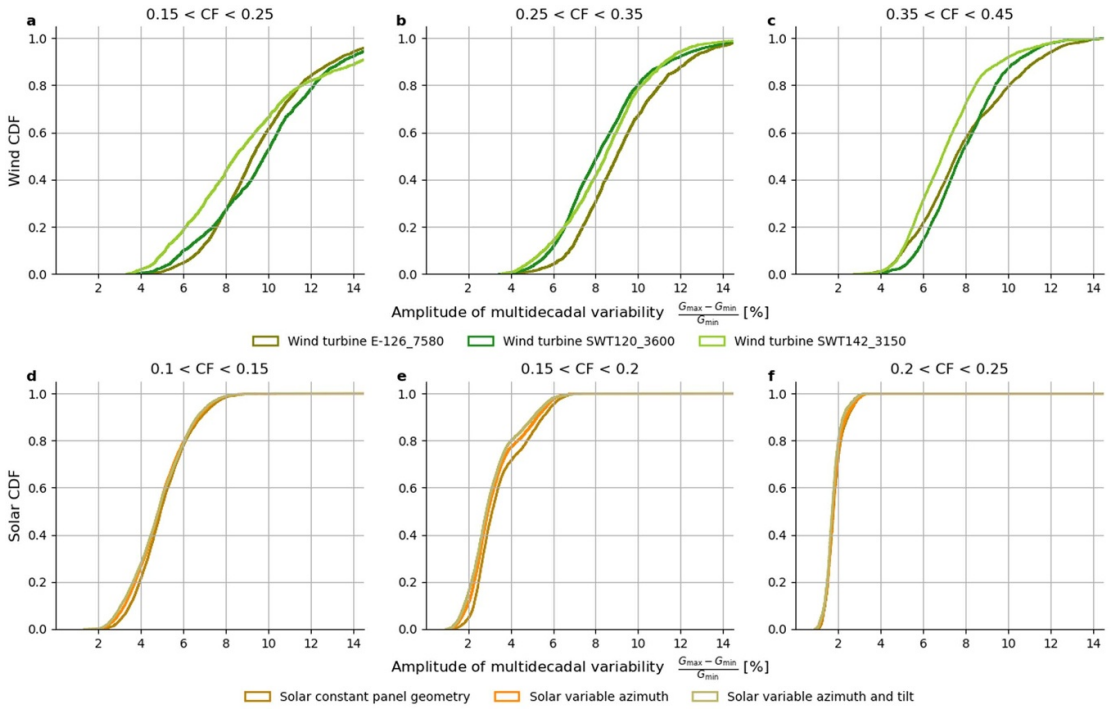

Figure 2. Cumulative density functions (CDFs) of the amplitude of multidecadal wind (a)–(c) and solar (d)–(f) variability. G_{max} (G_{min}) denote the maximum (minimum) of 20y running mean generation G. Columns denote different capacity factor brackets, in improving order from left to right, and we refer to them as low quality (a) and (d), medium quality (b) and (e), and high quality (c) and (f) sites. Each subplot displays the distribution of amplitudes over all sites that lie in the respective capacity factor bracket.

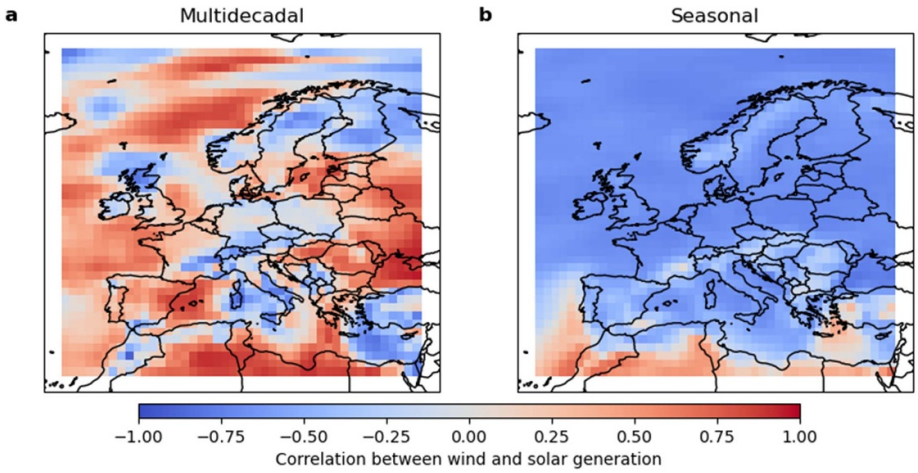

Figure 3. Correlation analysis between wind (SWT120_3600) and solar (constant panel geometry) generation on a multidecadal (a) and seasonal to interannual timescale (b). Multidecadal correlations are computed from the long-term 20y running mean filtered solar and wind generation covering 1917–1997 while seasonal correlations are based on the monthly mean solar and wind generation from 1980 to 2000.

3.2. Multidecadal local wind and solar generation complementarity is rare

The annual cycles of wind and solar power generation in Europe allow smoothing seasonal generation variability locally: high solar generation in the summer is complemented with relatively low wind generation; high wind generation in autumn and winter can compensate for reduced solar generation. This complementarity is reflected by pronounced negative correlations between monthly mean wind and solar generation everywhere on the continent (see figure 3), and it is robust for all turbines (cf figure F1).

Our results show, however, that wind and solar generation are mostly positively correlated on multidecadal timescales, implying that above average wind and solar generation tend to coincide. Even though some locations with negative correlations exist (e.g. in Italy, Scotland, and Eastern Scandinavia, see figure 3(b)), negative correlations are much less frequent on the multidecadal than the seasonal timescale. Local multidecadal co-variability is thus fundamentally different from seasonal co-variabiality and strategies to mitigate seasonal variability are likely ineffective on multidecadal scales.

3.3. Conflicting timescales in optimizing local wind shares

We quantify the potential to minimize generation variability locally by optimizing wind generation shares. As explained in the Methods section, the optimal wind share (i.e. wind to solar ratio) is derived for (a) twenty years of monthly mean data (referred to as seasonal due to the dominance of the seasonal cycle) and (b) eighty years of twenty-year running mean smoothed annual data. By isolating specific parts of the variability spectrum, this approach enables comparison of the seasonal timescale with the multidecadal timescale.

Overall, the amplitude of multidecadal variability is higher in seasonally optimized systems than in multidecadally optimized systems. While the amplitude lies between 2.5% and 5.0% with a mean around 4% in seasonally optimized systems, it drops to between 2.4% and 4% (mean approx. 3%) in multidecadally optimized systems (table 1).

Using the multidecadally optimal wind share, however, amplifies seasonal variability: the country-average amplitude of seasonal fluctuations almost doubles from 180% to 300% (supplementary table H1). Reductions of multidecadal variability thus increase seasonal variability and vice versa, highlighting that optimizing for one of these temporal scales conflicts with the other one.

We evaluate the optimal wind share on a country group level and find that the multidecadally optimal wind share is lower than the seasonally optimal one in seven out of nine groups. In other words, the multidecadal optimum favors solar power. This preference for solar power is caused by the lower amplitudes of multidecadal solar generation variability and the mostly positive correlations between wind and solar generation. Spain and Portugal are an extreme case: solar generation variability is particularly low, wind generation variability particularly high, and multidecadal correlations are positive virtually everywhere. This combination reduces the wind share to zero. Completely eliminating wind power, however, strongly conflicts with the seasonally optimal generation share of 57% and more than doubles the seasonal variability amplitude (see supplementary table H1). In other country groups, like the UK and Ireland, the drop in wind share is more modest because multidecadal correlations are partly negative and the difference in amplitudes of multidecadal wind and solar generation is smaller. Again, two out of nine country groups feature slightly increased wind shares

Table 1. Local wind share optimization. Displayed wind generation shares that minimize the combined wind and solar generation standard deviation evaluated for country combinations. The optimization is performed on a seasonal to interannual timescale (1980–2000) and a multidecadal timescale (20y running means covering 1917–1997). Shares are expressed in terms of installed capacity (i.e. α from equation (7)) and generation (i.e. long-term wind generation divided by longterm wind and solar generation) separately in two columns. The multidecadal amplitude $\frac{G_{max}-G_{min}}{G_{min}}$ is calculated using the wind shares that are seasonally optimal and multidecadally optimal.

	Seasonal share (%)		Multidecadal share (%)		Multidecadal variability amplitude (%)	
Country combination	Capacity	Generation	Capacity	Generation	Seasonal optimum	Multidecadal optimum
United Kingdom, Ireland	33	67	18	46	3.5	3.1
Portugal, Spain	42	57	0	0	4.2	2.4
France, Belgium, Netherlands	34	57	8	18	4.3	3.4
Germany, Denmark	34	61	13	31	4.2	3.8
Italy, Austria, Switzerland, Slovenia	28	43	34	50	2.6	2.7
Sweden, Norway	42	73	9	26	4.8	3.7
Poland, Czech Republic, Slovakia, Hungary	35	57	22	40	4.4	4.0
Lithuania, Latvia, Estonia, Finland	43	69	15	35	5.0	3.8
Greece, Bulgaria, Serbia, Croatia, Bosnia and Herzogovina, Romania, Albania	43	60	50	67	2.5	2.6

owing to negative correlations over larger parts of their domains, and thus benefit from local balancing potential.

Multidecadal fluctuations are generally stronger using seasonally optimized wind shares (e.g. Portugal and Spain, Sweden and Norway). However, in two cases, the fluctuations remain largely unchanged when either the seasonally optimized or multidecadally optimized wind shares are used (difference of 0.1% for Italy, Austria etc and Greece, Bulgaria etc). In the few close cases, seasonally optimal wind shares even lead to slightly lower multidecadal variability amplitudes. This seeming contradiction is rooted in our approach: we minimize the standard deviation and report the amplitude, which can deviate slightly.

When interpreting the percentages of the seasonal and multidecadal variability amplitudes, the different durations need to be considered. Given that 20 years contain 240 months, a monthly deviation must be 240 times stronger than a 20y mean deviation to induce the same energy deviation (in TWh). While the percentages are substantially higher for seasonal variability, the energy equivalents are higher for multidecadal variability.

We conclude that isolating the seasonal and multidecadal timescales leads to substantially different optimal wind and solar mixes and, in the multidecadal case, the optimization sometimes yields trivial solar-only solutions. In most country groups, mitigation of multidecadal variability is thus not a by-product of locally mitigating seasonal-scale variability.

3.4. Wind enables international multidecadal balancing

In addition to correlations and amplitudes of multidecadal changes, their spatio-temporal structure is important as it determines to which extent international transmission can be effective. The leading two EOF modes of long-term solar power generation reveal a spatially uniform evolution over the entire continent and explain most of the signal (85% of the variance, see figure E2). The first principle component strongly resembles dimming and brightening, with an inflection around 1980 and an early dimming in the 1940s (which is more pronounced in the ten-year running mean filtered data, see figure E3(e)), and is therefore backed up by a known physical phenomenon. Since these changes are largely uniform and synchronous across the continent, attempts to smooth multidecadal *solar* variability via international transmission are ineffective. Excluding locations further north than 70° (about Tromso, Norway), which excludes areas heavily affected from sea-ice loss and consequently changes in albedo and backscattering, demonstrates robustness of our results to domain redefinition (figure E4).

Investigating wind and solar power jointly, however, reveals that the leading multivariate EOF (MEOF) wind modes are multipoles, that is, exhibit

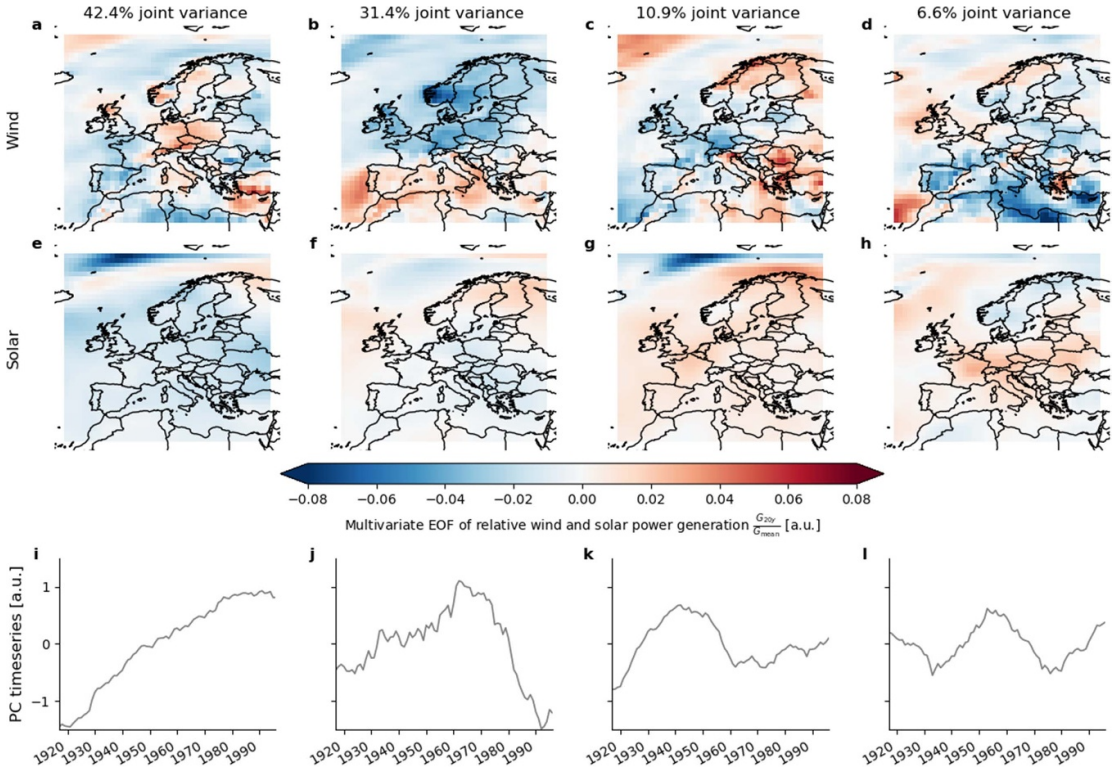

Figure 4. Multivariate EOF analysis of multidecadal wind and solar generation. The first line shows the wind patterns (a)–(d), the second line illustrates the solar patterns (e)–(h), and the last line gives the corresponding principle component timeseries (i)–(l). The explained joint variance per MEOF is given in the titles of (a)–(d) (e.g. the wind and solar patterns and the principle component timeseries in the first column (a), (e), (i) explain 42.4% of joint variance). MEOF analysis is performed on the 20y running mean normalized solar (constant panel geometry) and wind generation (E-126_7580). Note that the MEOFs and the PC timeseries have arbitrary units, only their product has the same units as $\frac{G_{20y}}{G_{mean}}$.

spatial variability which could be exploited to balance power supply (see figure 4). For instance, the first wind MEOF has a different sign in Germany, Poland, and the Czech Republic than in France and the Iberian Peninsula, indicating that above average wind generation in one country group corresponds to below average generation in the other. The second MEOF has a clear North-South divide, and the next two MEOFs also feature domains of different signs, pointing towards international balancing potential. MEOFs for the other turbines are qualitatively identical, implying that the spatio-temporal structure of large scale variability is insensitive to the specific turbine choice (figures G1 and G2).

We quantify the effect of multidecadal wind complementarity on balancing potentials by computing the amplitude reductions that can be achieved through electricity transmission between the country groups (figure 5). Using the currently installed per-country capacities (IRENA 2020), we find that the continent as a whole and seven out of nine country groups would benefit from multidecadal international balancing (figure 5(a)). Cutting off the 'Portugal and Spain' country group from the continental transmission system would increase the multidecadal amplitude both on the Iberian peninsula and in the rest of the continent compared to the full European region (shown by amplitude increases relative to the purple line). In many other country groups, we find a strong amplitude increase if the group is cut off from transmission, along with a mild decrease in the continent-wide amplitude. In other words, the cost of self-sufficiency, in terms of multidecadal variability, is high for most individual country groups. One of the groups that does not benefit on the multidecadal scale (IT, AU, CH, SI) still benefits from reduced variability on the seasonal scale, making inter-country transmission appealing in any case (SI figure I1(a)). The other group that does not benefit on the multidecadal scale is located in South-Eastern Europe (including Greece and Bulgaria), and currently only has limited wind and solar installations, each corresponding to around 4% of European capacity. As this country group catches up with the others in terms of installed capacity, the isolated multidecadal amplitude approaches the continental one (SI figure I2(b)).

Moreover, comparing hypothetical wind-only or solar-only systems, we find that the amplitudes of multidecadal solar and wind variability are similar on a continental scale despite the substantial local differences. In fact, both the current wind and solar fleets feature the same amplitude of 3.5% given sufficient inter-country group transmission (figure 5(b)),

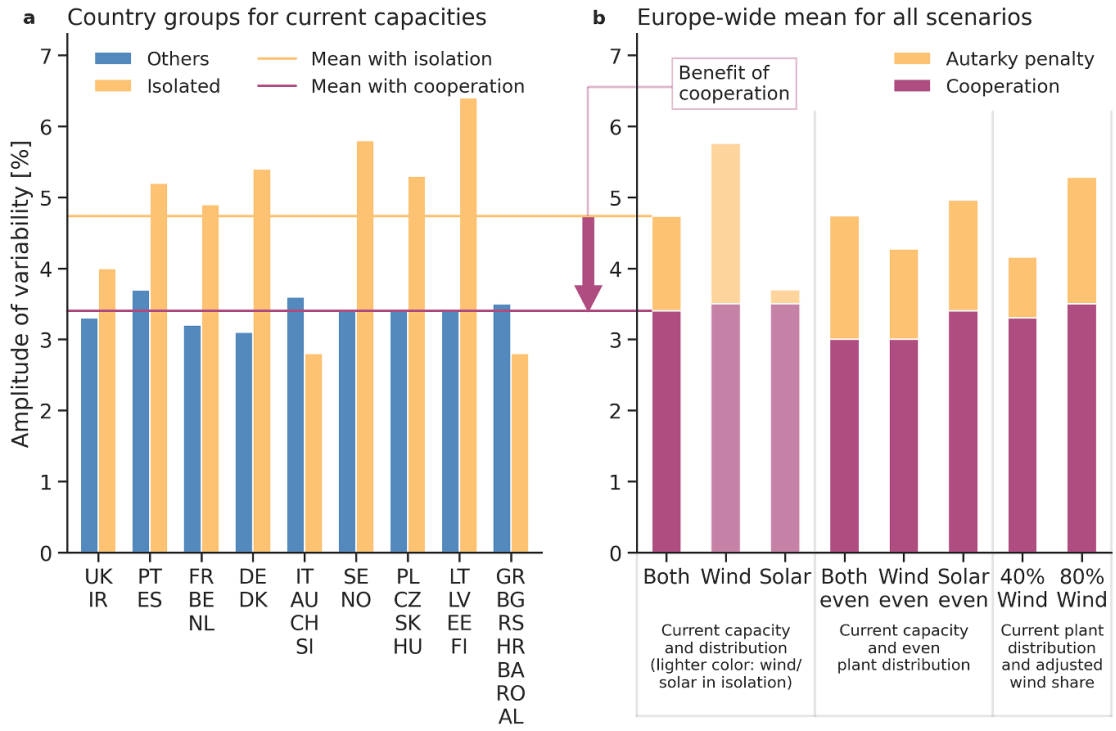

Figure 5. Multidecadal spatial balancing potential of wind and solar generation. The amplitude of multidecadal variability is given per country group for the currently installed wind and solar capacities (a), and for the entire continent using different scenarios (b). 'Others' denotes an interconnected European system excluding a country group and 'isolated' refers to the case of no transmission between a country group and the rest of Europe. 'Mean with isolation' is the (capacity-weighted) mean of all variability amplitudes, 'mean with cooperation' denotes the case of unlimited transmission and we refer to the difference between them as 'autarky penalty'. As visualized by the arrow in (a), the difference can likewise be interpreted as the 'benefit of cooperation'. The scenarios in (b) include the current capacity layout ('current capacity and distribution'), altered spatial distributions that leave the continental wind and solar share unchanged ('current capacity and even plant distribution'), and altered continental wind and solar shares with unchanged spatial distributions ('current plant distribution and adjusted wind share'). Wind shares of 40% and 80% correspond to a 20% deviation from the current 60% share. Scenarios generally include both wind and solar generation with the exception of the current wind and current solar scenarios which consider the respective technology in isolation.

emphasizing that wind generation can be equally reliable as solar generation on long timescales and over large geographic areas. The autarky penalty (i.e. the difference between an interconnected and isolated power system), however, is one order of magnitude larger for wind than for solar power dominated systems (2.3% vs. 0.2%). While current wind capacity is highly clustered, with more than one third installed in Germany and Denmark, uniform capacity distribution across the continent would reduce continental multidecadal variability further to 3%, making spatially diversified combined systems less vulnerable than those relying on solar power only. Continentally uniform solar generation distribution, in contrast, leaves the continental amplitude unchanged and even mildly increases the isolation penalty.

4. Discussion

Four strategies to cope with with multidecadal wind and solar generation variability are imaginable: building power systems whose generation is invariant under multidecadal climate variability (e.g. through optimized portfolios and international transmission), relying on flexibility provided by other parts of the energy system (e.g. through electricity storage, backup power plants, or sector coupling), installing wind and solar overcapacity, or anticipating climate conditions over the next one or two decades and adapting capacity expansion accordingly. While there is potential for decadal-scale predictions in the North Atlantic area (e.g. Årthun *et al* 2017, Smith *et al* 2020), and the translation of seasonal climate predictions to energy-relevant variables has been demonstrated (Clark *et al* 2017), it remains unclear if and when this last option will become reliable enough to inform multi-billion Euro investments in energy infrastructure. Installing overcapacity on the order of 5% may be the simplest and most robust approach, but comes with potentially prohibitive additional costs, loads on transmission lines, and land requirements. Equally, the storage or flexibility potentials required to balance a relative generation shortfall lasting twenty or more years are likely to be cost-prohibitive. However, identifying capacity layouts that are less or not at all affected by multidecadal climate variability is a winning strategy in any case: it minimizes both risks and costs, and still leaves the

possibility open to also rely on the other options at a later stage. Consequently, minimizing multidecadal fluctuations should be added to design criteria for highly renewable power systems.

It is important to note that the amplitudes of multidecadal variability reported in this study are of the same magnitude or larger than climate change impacts on renewables calculated using climate model output for the 21st century (Pryor and Barthelmie 2010, Jerez *et al* 2015, 2019, Reyers *et al* 2016, Tobin *et al* 2016, 2018, Wohland *et al* 2017, Müller *et al* 2019). For example, Tobin *et al* (2016) find wind farm yield changes of less than 5% for most regions and models and Müller *et al* (2019) report annual PV potential changes between -6% and +3%. The similar amplitudes of presumably forced signals and long-term climate variability thus further complicate the separation of signals (i.e. climate change impacts) from noise (i.e. manifestations of climate variability), see Hawkins and Sutton (2009). In order to reliably attribute climate change impacts on renewables, we need more in-depth investigations to clarify the extent to which multidecadal wind and solar generation variability is captured in current global climate models, for example, based on unforced long-term simulations (Rugenstein *et al* 2019).

We here conducted the first century-scale and continent-wide wind and solar generation assessment with uninterrupted and plausibility-checked historic climate input data. Climate-induced multidecadal renewable generation variability has an amplitude exceeding 10% for wind power generation in many locations and different correlations between wind and solar generation than on seasonal timescales and could therefore threaten power system stability in future highly renewable power systems if it remains unaddressed. It is unlikely to be manageable with any existing or foreseen storage technology given the long storage durations. However, incorporating long-term climate information in energy system planning, in particular with respect to relative wind and solar shares and strategic siting of wind farms, would permit a substantial reduction of multidecadal variability, thereby minimizing the need for renewable overcapacity or backup generation infrastructure. Our long-term wind and solar generation data is openly available to enable further research which could, for instance, investigate spectral properties, extremes, or the impacts on a sector-coupled energy system model.

Code and data availability

We provide three hourly ensemble mean wind and solar power generation timeseries and the country group timeseries via the data sharing platform zenodo (doi: https://doi.org/10.5281/zenodo.4280851). The code is written in Python and is available on github (https://github.com/jwohland/wind_n_solar). Input data from NOAA-CIRES and ECMWF are available free of charge online, for example, via https://portal.nersc.gov/archive/home/projects/incite11/www/20C_Reanalysis_version_3/everymember_anal_netcdf/mnmean/UGRD100m and https://apps.ecmwf.int/datasets/data/cera20c-enda/levtype = sfc/type = fc/.

Acknowledgments

J W wants to thank Gil Compo and NOAA-CIRES in general for access to the NERSC computing infrastructure. J W is funded through an ETH Postdoctoral Fellowship and acknowledges support from the ETH foundation and the Uniscientia foundation. S P acknowledges funding from the SENTINEL project of the European Union's Horizon 2020 research and innovation programme under Grant Agreement No. 83708. Numerical analysis was performed on the ETH Zürich cluster Euler. The authors want to thank ECMWF and NOAA-CIRES for making CERA20C and 20CRv3 publicly available. Support for the Twentieth Century Reanalysis Project dataset is provided by the U.S. Department of Energy, Office of Science Biological and Environmental Research (BER) program, by the National Oceanic and Atmospheric Administration Climate Program Office, and by the NOAA Physical Sciences Laboratory.

Competing interests

The authors declare that no competing interests exist.

ORCID iDs

Jan Wohland https://orcid.org/0000-0001-8336-0009
David Brayshaw https://orcid.org/0000-0002-3927-4362
Stefan Pfenninger https://orcid.org/0000-0002-8420-9498

References

Årthun M, Eldevik T, Viste E, Drange H, Furevik T, Johnson H L and Keenlyside N S 2017 Skillful prediction of northern climate provided by the ocean *Nat. Commun.* **8** 15875

Befort D J, Wild S, Kruschke T, Ulbrich U and Leckebusch G C 2016 Different long-term trends of extra-tropical cyclones and windstorms in ERA-20C and NOAA-20CR reanalyses: extra-tropical cyclones and windstorms in 20th century reanalyses *Atmos. Sci. Lett.* **17** 586–95

Bett P E, Thornton H E and Clark R T 2017 Using the twentieth century reanalysis to assess climate variability for the European wind industry *Theor. Appl. Climatol.* **127** 61–80

Bloomfield H C *et al* 2021 The importance of weather and climate to energy systems: a workshop on next generation challenges in energy–climate modeling *Bull. Am. Meteorol. Soc.* **102** E159–67

Bloomfield H C, Brayshaw D J, Shaffrey L C, Coker P J and Thornton H E 2016 Quantifying the increasing sensitivity of power systems to climate variability *Environ. Res. Lett.* **11** 124025

Bloomfield H C, Shaffrey L C, Hodges K I and Vidale P L 2018 A critical assessment of the long-term changes in the wintertime surface Arctic Oscillation and Northern hemisphere storminess in the ERA20C reanalysis *Environ. Res. Lett.* **13** 094004

Cardone V J, Greenwood J G and Cane M A 1990 On trends in historical marine wind data *J. Clim.* **3** 113–27

Clark R T, Bett P E, Thornton H E and Scaife A A 2017 Skilful seasonal predictions for the European energy industry *Environ. Res. Lett.* **12** 024002

Collins S, Deane P, Gallachóir O B, Pfenninger S and Staffell I 2018 Impacts of inter-annual wind and solar variations on the European power system *Joule* **2** 2076–90

Dawson A 2016 eofs: a library for EOF analysis of meteorological, oceanographic and climate data *J. Open Res. Softw.* **4** e14

European Commission 2019 *The European Green Deal*

Farneti R 2017 Modelling interdecadal climate variability and the role of the ocean: modelling interdecadal climate variability and the role of the ocean *Wiley Interdiscip. Rev.: Clim. Change* **8** e441

González-Aparicio I, Monforti F, Volker P, Zucker A, Careri F, Huld T and Badger J 2017 Simulating European wind power generation applying statistical downscaling to reanalysis data *Appl. Energy* **199** 155–68

Grams C M, Beerli R, Pfenninger S, Staffell I and Wernli H 2017 Balancing Europe's wind-power output through spatial deployment informed by weather regimes *Nat. Clim. Change* **7** 557–62

Haas S, Schachler B and Krien U 2019 Windpowerlib—a python library to model wind power—v.0.2.0 (https://doi.org/10.5281/zenodo.3403360)

Hawkins E and Sutton R 2009 The potential to narrow uncertainty in regional climate predictions *Bull. Am. Meteorol. Soc.* **90** 1095–108

Heide D, von Bremen L, Greiner M, Hoffmann C, Speckmann M and Bofinger S 2010 Seasonal optimal mix of wind and solar power in a future, highly renewable Europe *Renew. Energy* **35** 2483–9

IRENA 2020 *Renewable Capacity Statistics 2020* (Abu Dhabi)

Jerez S *et al* 2015 The impact of climate change on photovoltaic power generation in Europe *Nat. Commun.* **6** 10014

Jerez S, Tobin I, Turco M, Jiménez-Guerrero P, Vautard R and Montávez J 2019 Future changes, or lack thereof, in the temporal variability of the combined wind-plus-solar power production in Europe *Renew. Energy* **139** 251–60

Keenlyside N S, Ba J, Mecking J, Omrani N-E, Latif M, Zhang R and Msadek R 2015 North Atlantic multi-decadal variability—mechanisms and predictability *World Scientific Series on Asia-Pacific Weather and Climate* vol 6 (Singapore: World Scientific) pp 141–57

Knorr K 2016 Modellierung von raumzeitlichen Eigenschaften der Windenergieeinspeisung für wetterdatenbasierte Windleistungssimulationen Dissertation Fachbereich Elektrotechnik/Informatik der Universität Kassel

Laloyaux P *et al* 2018 CERA-20C: a coupled reanalysis of the twentieth century *J. Adv. Model. Earth Syst.* **10** 1172–95

Meucci A, Young I R, Aarnes O J and Breivik O 2020 Comparison of wind speed and wave height trends from twentieth-century models and satellite altimeters *J. Clim.* **33** 611–24

Müller B, Wild M, Driesse A and Behrens K 2014 Rethinking solar resource assessments in the context of global dimming and brightening *Sol. Energy* **99** 272–82

Müller J, Folini D, Wild M and Pfenninger S 2019 CMIP-5 models project photovoltaics are a no-regrets investment in Europe irrespective of climate change *Energy* **171** 135–48

Pfenninger S and Staffell I 2016 Long-term patterns of European PV output using 30 years of validated hourly reanalysis and satellite data *Energy* **114** 1251–65

Pryor S and Barthelmie R 2010 Climate change impacts on wind energy: a review *Renew. Sustain. Energy Rev.* **14** 430–7

Reyers M, Moemken J and Pinto J G 2016 Future changes of wind energy potentials over Europe in a large CMIP5 multi-model ensemble *Int. J. Climatol.* **36** 783–96

Rodríguez R A, Becker S, Andresen G B, Heide D and Greiner M 2014 Transmission needs across a fully renewable European power system *Renew. Energy* **63** 467–76

Rugenstein M *et al* 2019 LongRunMIP: motivation and design for a large collection of millennial-length AOGCM simulations *Bull. Am. Meteorol. Soc.* **100** 2551–70

Santos-Alamillos F J, Brayshaw D J, Methven J, Thomaidis N S, Ruiz-Arias J A and Pozo-Vázquez D 2017 Exploring the meteorological potential for planning a high performance European electricity super-grid: optimal power capacity distribution among countries *Environ. Res. Lett.* **12** 114030

Slivinski L C *et al* 2019 Towards a more reliable historical reanalysis: improvements for version 3 of the twentieth century reanalysis system *Q. J. R. Meteorol. Soc.* **145** 2876–908

Smith D M *et al* 2020 North Atlantic climate far more predictable than models imply *Nature* **583** 796–800

Staffell I and Pfenninger S 2016 Using bias-corrected reanalysis to simulate current and future wind power output *Energy* **114** 1224–39

Storch H V and Zwiers F W 1999 *Statistical Analysis in Climate Research* (Cambridge: Cambridge University Press)

Sweerts B, Pfenninger S, Yang S, Folini D, van der Zwaan B and Wild M 2019 Estimation of losses in solar energy production from air pollution in China since 1960 using surface radiation data *Nat. Energy* **4** 657–63

Tobin I *et al* 2016 Climate change impacts on the power generation potential of a European mid-century wind farms scenario *Environ. Res. Lett.* **11** 034013

Tobin I, Greuell W, Jerez S, Ludwig F, Vautard R, van Vliet M T H and Bréon F-M 2018 Vulnerabilities and resilience of European power generation to 1.5 °C, 2 °C and 3 °C warming *Environ. Res. Lett.* **13** 044024

van den Dool H 2007 *Empirical Methods in Short-Term Climate Prediction* (Oxford: Oxford University Press)

van der Wiel K, Stoop L, van Zuijlen B, Blackport R, van den Broek M and Selten F 2019 Meteorological conditions leading to extreme low variable renewable energy production and extreme high energy shortfall *Renew. Sustain. Energy Rev.* **111** 261–75

Vautard R, Cattiaux J, Yiou P, Thépaut J-N and Ciais P 2010 Northern hemisphere atmospheric stilling partly attributed to an increase in surface roughness *Nat. Geosci.* **3** 756–61

Ward M N and Hoskins B J 1996 Near-surface wind over the global ocean 1949–1988 *J. Clim.* **9** 1877–95

Wever N 2012 Quantifying trends in surface roughness and the effect on surface wind speed observations: surface roughness and wind speed trends *J. Geophys. Res.: Atmos.* **117** D11104

Wild M 2016 Decadal changes in radiative fluxes at land and ocean surfaces and their relevance for global warming *Wiley Interdiscip. Rev.: Clim. Change* **7** 91–107

Williams P D *et al* 2017 A census of atmospheric variability from seconds to decades *Geophys. Res. Lett.* **44** 11,201–11,211

Wohland J, Brayshaw D, Bloomfield H and Wild M 2020 European multidecadal solar variability badly captured in all centennial reanalyses except CERA20C *Environ. Res. Lett.* **15** 104021

Wohland J, Omrani N E, Keenlyside N and Witthaut D 2019b Significant multidecadal variability in German wind energy generation *Wind Energy Sci.* **4** 515–26

Wohland J, Omrani N, Witthaut D and Keenlyside N S 2019a Inconsistent wind speed trends in current twentieth century reanalyses *J. Geophys. Res.: Atmos.* **124** 1931–40

Wohland J, Reyers M, Weber J and Witthaut D 2017 More homogeneous wind conditions under strong climate change decrease the potential for inter-state balancing of electricity in Europe *Earth Syst. Dyn.* **8** 1047–60

Zeng Z *et al* 2019 A reversal in global terrestrial stilling and its implications for wind energy production *Nat. Clim. Change* **9** 979–85